RNA-binding protein Syncrip regulates Starvation-Induced Hyperactivity in *adult Drosophila*

Wanhao Chi[1,2,*], Wei Liu[3], Wenqin Fu[2], Ellie S. Heckscher[1,4,5], Xiaoxi Zhuang[1,2,5,*]

Abstract

How to respond to starvation determines fitness. One prominent behavioral response is increased locomotor activities upon starvation, also known as Starvation-Induced Hyperactivity (SIH). SIH is paradoxical as it promotes food seeking but also increases energy expenditure. Either too much or too little SIH would impair fitness. Despite its importance, the genetic contributions to SIH as a behavioral trait remains unexplored. Here, we examined SIH in the *Drosophila melanogaster* Genetic Reference Panel (DGRP) and performed genome-wide association studies. We identified 27 significant loci, corresponding to 18 genes, significantly associated with SIH in adult *Drosophila*. Gene enrichment analyses indicated that genes encoding ion channels and mRNA binding proteins (RBPs) were most enriched in SIH. We are especially interested in RBPs because they provide a potential mechanism to quickly change protein expression in response to environmental challenges. Using RNA interference, we validated the role of *Syp* in regulating SIH. *Syp* encodes Syncrip, an RBP. While ubiquitous knockdown of *Syp* led to lethality during development, adult flies with neuron specific *Syp* knockdown were viable and exhibited decreased SIH. Using the Temporal and Regional Gene Expression Targeting (TARGET) system, we further confirmed the role of Syp in adult neurons in regulating SIH. Lastly, RNA-seq analyses revealed that *Syp* was alternatively spliced under starvation while its expression level was unchanged. Together, this study not only demonstrates genetic contributions to SIH as an important behavioral trait but also highlights the significance of RBPs and post-transcriptional processes in regulating SIH.

Keywords

Genome-wide association study, DGRP, Starvation-Induced Hyperactivity, RNA-binding Protein, RNA-seq

[1] *Committee on Genetics, Genomics Systems Biology* [2] *Department of Neurobiology, University of Chicago, Chicago, IL 60637, USA*
[3] *Department of Environmental Health, School of Public Health, China Medical University, Shenyang 110122, P.R. China*
[4] *Department of Molecular Genetics and Cell Biology, University of Chicago, Chicago, IL 60637, USA*
[5] *Grossman Institute for Neuroscience, Quantitative Biology and Human Behavior, University of Chicago, Chicago, IL 60637, USA*
*__Corresponding authors__: wchi1@bsd.uchicago.edu; xzhuang@bsd.uchicago.edu

Introduction

Animals living in the natural environment often experience periods of starvation, and they have thus developed different physiological and behavioral strategies to respond to starvation [1, 2]. One well-documented behavioral response is Starvation-Induced Hyperactivity (SIH), that is, animals will increase their locomotor activity upon starvation [3]. SIH has been observed in both flies [4, 5, 6, 7, 8, 9] and mammals [10, 11, 12], suggesting that this behavior is evolutionarily conserved. From the viewpoint of energy gain and expenditure, SIH seems paradoxical. On one hand, it facilitates food acquisition and energy intake when food is available [7]; on the other hand, it increases energy expenditure and makes starved animals even more vulnerable when food is not available [4]. Therefore, genetic dispositions to either too much or too little SIH would impair fitness depending on the environment. However, the genetic contributions to SIH as a behavioral trait remains unexplored.

Recent studies suggest that SIH is highly regulated. A number of genes have been shown to regulate SIH in adult *Drosophila*, including genes encoding energy sensors [5, 6], neuropeptides/neuropeptide receptors [4, 8], and neurotransmitters [7]. Recently, *dG9a* was shown to regulate SIH in adult *Drosophila* [9]. Gene *dG9a* encodes a histone methyltransferase, suggesting that SIH is also regulated at the epigenetic level. In addition, post-transcriptional modifications, especially alternative pre-mRNA splicing, has been shown to be effective for cells and animals to quickly respond to starvation as well as other stresses [13, 14, 15]. However, whether or not alternative pre-mRNA splicing plays a role in SIH has not been reported.

In this study, we first set out to determine whether SIH varied in a population of *Drosophila melanogaster* with diversified genetic background. We used the *Drosophila melanogaster* Genetic Reference Panel (DGRP). The DGRP consists of 205 inbred wild-type strains derived from wild population that was collected from the Raleigh, North Carolina, USA [16, 17]. It is a recently established community resource and has been used to examine the genetic basis of more than 60 quantitative traits [18]. We assayed 198 DGRP strains, quantified SIH in each strain, and confirmed a significant genetic contribution

to SIH. We then performed genome-wide association studies and identified 27 significant loci from 18 genes associated with SIH. We found that genes with ion channel activities and mRNA binding activities were especially enriched in SIH. Using RNA interference, we validated the role of a gene encoding an RNA-binding protein Syncrip (Syp) [19] in neurons in regulating SIH. Using the Temporal and Regional Gene expression Targeting (TARGET) system [20], we further confirmed the role of *Syp* in adult neurons in regulating SIH. Lastly, using RNA-seq, we found that *Syp* was alternatively spliced under starvation while its expression level remained unchanged.

Methods

Drosophila stocks

The *Drosophila melanogaster* Genetic Reference Panel (DGRP) strains were from the Bloomington Drosophila Stock Center (BDSC). The UAS- *Syp* RNAi lines (#33011, #33012) and the genetic control line were from the Vienna Drosophila Resource Center (VDRC). The *actin*-Gal4 (#4414) and the pan-neuronal driver *nSyb*-Gal4 (#51635) were from the BDSC. Unless stated otherwise, all flies were reared on the standard cornmeal medium from FlyKitchen at the University of Chicago at 25°C under a 12-hr:12-hr light: dark cycle with the light on at 06:00 and off at 18:00.

Locomotor assay setup

Male flies, 1 to 3 d old, were anesthetized briefly and transferred into activity tubes filled with the standard cornmeal medium where they were allowed to recover from CO2. One day later, flies were randomly separated into two groups. Flies in the first group were transferred into activity tubes filled with 4% sucrose plus 5% yeast in 1% agar (food condition), and flies in the second group were transferred into activity tubes filled with 1% agar only (starvation condition). The other end of activity tubes was inserted with a small cotton ball to allow air exchange for the fly and also to prevent fly from escaping. The locomotor activity of each fly was monitored using the Drosophila Activity Monitor (DAM2, Trikinetics Inc.). Unless stated otherwise, the assay chamber was maintained at 25°C under a 12-hr:12-hr light: dark cycle with the light on at 06:00 and off at 18:00. The start point on the plots is the light off point, which is 18:00 on the setup day, which is about 6-7 hours after flies were transferred to the activity tubes. We used 8 flies per condition per genotype for screening. The number of flies in other experiments was indicated in the text.

Data analysis of the locomotor responses to starvation

Infrared beam breaks per 30-minute interval from two conditions were averaged and plotted as a function of time point for each strain. The total activity of each fly from a 12-hour period (either daytime or nighttime) in each condition was first summed, and the activity difference between the two conditions was then calculated. Since flies were monitored for a total of sixty hours, there were five DAs. The largest DA among five DAs was referred to as DA of each fly. The averaged DA from 8 flies was used to represent the strain DA.

Starvation Resistance

Starvation Resistance is represented by the time point (0-120) when all eight flies under starvation were dead. The death of a fly was inferred from the activity data such that there were no beam crosses. In the case of all flies survived to the last time point, an index of 121 was used.

Genome-wide association analysis

Genome-wide association analysis on SIH was performed using the DGRP analysis pipeline at http://dgrp2.gnets.ncsu.edu [16, 17]. Briefly, each raw dataset was first adjusted for the Wolbachia infection and the inversion with a linear model where the raw dataset as the response variable and the infection status and five major inversion polymorphisms as covariates (Table S3). Residuals from this linear model were then used as response variable to fit a mixed linear model: $Y = \mu + G + r$, where μ is the overall population mean for each trait, G is the effect of SNPs or INDELs being tested, and r is a polygenic component with covariance between lines determined by their genome relationship [17]. A nominal *P*-value threshold of $P < 1 \times 10^{-5}$ was used for declaring SNPs or INDELs to be significantly associated with trait variation.

Gene enrichment analysis

The web-based enrichment analysis tool FlyEnrichr [21, 22] was applied to evaluate the list of candidate genes, and to obtain a set of enriched functional annotations in three domains: biological process (BP), cellular component (CC), and molecular function (MF) [23] or in KEGG (Kyoto Encyclopedia of Genes and Genomes) pathways [24]. GO (gene ontology) or KEGG terms with $P < 0.05$ (after Benjamini-Hochberg correlation) were listed in Tables S5 and S8.

Western blotting

For the Gal80^{ts} experiment, a group of 25-30 male flies, 1 to 3 d old, were reared on the standard cornmeal medium at either 18°C or 31°C for two days. For the protein level of Syp in w^{1118} flies under either food or starvation conditions, a group of 25-30 male flies, 1 to 3 d old, were maintained in either food or starvation conditions at the room temperature for one day. The total protein from adult heads was then extracted and quantified. A total of 50 μg protein from each sample was loaded for SDS-PAGE. Separated proteins were electrophoretically transferred to the PVDF membrane. After blocking, the membrane was incubated with primary antibodies (Guinea pig anti-Syp 1:2000 Ilan Davis, UK; Mouse anti-tubulin 1:500 Developmental Studies Hybridoma Bank, DSHB) and then the secondary antibodies (peroxidase-labeled anti-Guinea pig IgG 1:10,000, Sigma; peroxidase-labeled anti-mouse IgG 1:10,000, Jackson ImmunoResearch Laboratories). Signals were detected with enhanced chemiluminescence (Thermo-Scientific).

RNA extraction

A group of 30 male flies, 1 to 3 d old, were maintained under either food or starvation conditions for one day. Four biological samples were collected for each condition. Total RNA was extracted from heads using RNA extraction kit (Zymo Research). After the removal of genomic DNA (DNA-free kit, AMBION), total RNA was quantified using a NanoDrop spectrophotometer (Thermo Scientific), and the concentrations of total RNA were then diluted to 100 ng/μL.

RNA sequencing and data analysis

RNA sequencing was performed in the Genomics Core Facility at the University of Chicago. Briefly, the integrity of total RNA was assessed using a bioanalyzer 2100 (Agilent), and poly(A)+ RNA-seq libraries were then prepared from each sample, multiplexed, and sequenced by 100-bp paired ends using Illumina HiSeq4000 sequencer (Figures S4 and S5). Sequencing was duplicated using two flow cells. A total of 15-30 million reads were generated for each library per sequencing batch. Sequencing quality was assessed using FastQC [25], and the mean quality score ranges from 38.84 to 39. Raw sequencing reads from each group (treatments + biological replicates + sequencing batches) were individually mapped to the Drosophila genome (v6.22) using STAR (v2.6.1b) [26]. About 95% of raw reads from each sample were uniquely mapped to the genome. Each bam file was then processed using ASpli [27] to obtain differentially expressed genes and thereby to access the sequencing batch effect (Figure S6). Since results from two sequencing batches are highly correlated (ρ = 0.99, P < 2.2e-16, Pearson correlation test), we merged two sequencing bam files from the same sample using samtools [28] for downstream analyses. Alternative splice variants were analyzed using Leafcutter [29].

qRT-PCR

The cDNAs were synthesized using SMARTScribe Reverse Transcription Kit (TaKaRa). Two pairs of primers that targeted either both exons b and c or exon b only (Figure 5A) were used to amplify these two exons. Primer sequences of the first pair of primers are: 5′- TTC ACC GAT GGC TAG TGG AC and 5′- GTT GGC CAA CGA CTC TGC CA, and primer sequences of the second pair of primers are: 5′- TTC GGT TTC TCG GAC TAT CG and 5′- CCA CCG TTC GGG TAA TCA TA. One pair of primers that targeted the house-keeping gene *ribosomal protein 49* (*rp49*) was used as the internal control for qPCR. Primer sequences are: 5′- GCT AAG CTG TCG CAC AAA TG and 5′- GTT CGA TCC GTA ACC GAT GT.

Correlation, quantitative genetic, and statistical analyses

All analyses were performed using the statistical software R v3.6.1 (http://www.r-project.org). Pearson correlation test was used for correlation analyses. Other statistical tests were indicated in the text or figure legends. The broad-sense heritability (H^2) of SIH was computed as $H^2 = \sigma^2{}_G/(\sigma^2{}_G + \sigma^2{}_E)$, where $\sigma^2{}_G$ is the among-line variance component and $\sigma^2{}_E$ is the error variance.

Results

Natural variation in Starvation-Induced Hyperactivity across DGRP

To study the natural variation in Starvation-Induced Hyperactivity (SIH), we monitored the locomotor activity of 198 strains in the *Drosophila melanogaster* Genetic Reference Panel (DGRP) [16, 17] under either food or starvation conditions in the Drosophila Activity Monitor for three days (Figure S1; See Methods). DGRP consists of 205 inbred strains that were derived from wild flies from the Raleigh, NC, USA. We excluded those strains that did not breed well.

The locomotor activity of each strain under either food or starvation conditions was plotted as a function of time, sixty hours in total. Representative plots are shown in Figure 1A. We observed that, under a 12-hr:12-hr day-night condition and with the presence of food, all strains showed typical bimodal activity peaks, a day-night rhythm governed by the circadian system [30] (black lines in Figure 1A). Such rhythmic activities were disrupted by food deprivation in most strains. Starved flies became persistently active and the hyperactivity could occur in either day or night (red lines in Figure 1A). There were exceptions as some strains did not show obvious SIH (See a representative strain in Figure 1A, the bottom panel).

To quantify SIH, we used the total activity during the 12-hr nighttime or daytime, and then calculated the activity difference (Delta Activity, DA) between the starvation condition and the food condition (See Methods for details). Since activities were recorded for a total of sixty hours (3 nights and 2 days), a total of five DA values were obtained accordingly. To compare the DAs among 198 trains in the DGRP, we used the largest DA among five DAs to represent the strain DA. An absolute activity difference instead of a relative activity difference was used because we did not see a correlation between DA and baseline activity (ρ = 0.046, P = 0.519; Table S1), suggesting that DA was not increased proportionally to the baseline level. A summary plot of the largest DA (DA hereafter) across 198 strains was shown in Figure 1B. DA ranged from 93.61 $\pm$ 72.22 to 2101.91 $\pm$ 150.76 with a broad sense heritability of H^2 = 0.38 (Tables S1 and S2). Thus, SIH varies among DGRP strains and it has a strong genetic basis.

Starvation-Induced Hyperactivity is negatively correlated with Starvation Resistance

Previous studies showed that flies with reduced SIH survived longer under starvation [5, 6], suggesting that SIH is negatively correlated with Starvation Resistance (SR). To examine whether this relationship could also be observed in DGRP strains which were derived from a natural population, we did a correlation analysis between SIH and SR. We found that SIH was indeed negatively correlated with SR, but the correlation was not particularly strong (ρ = -0.231, P = 1.04

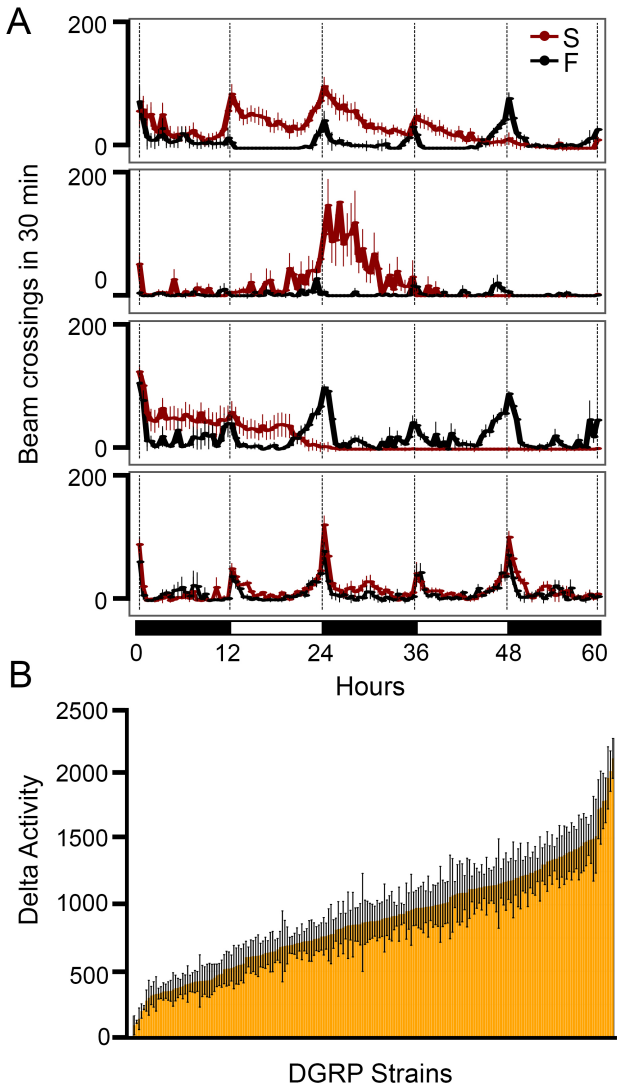

Figure 1. Natural variation of Starvation-Induced Hyperactivity in the DGRP. (A) Representative plots of locomotor activity responses to starvation. Beam crosses in 30 min were plotted as a function of time. Black lines represent activities under the food condition (F) and red lines represent activities under the starvation condition (S). Black and white bars at the bottom of panel A represent night and day cycles, respectively. Each plot was from one DGRP strain (n = 8 per condition). (B) Natural variation occurred in SIH across DGRP. Error bars represent SEM.

e-03; n =198). Studies have demonstrated that SIH resembles foraging behavior [7]. Previously, we have studied the survival rates of DGRP strains in a foraging environment [31]. Thus, we further examined the correlation relationship between SIH and the foraging survival rates of DGRP strains. We did not find any correlation between them (ρ = -0.073, P = 0.309; n = 197), which is not too surprising as the beneficial or detrimental effects of SIH may well depend on the specific environmental conditions.

GWA analysis of Starvation-Induced Hyperactivity

We next performed genome-wide association analysis using the DGRP analysis pipeline (http://dgrp2.gnets.ncsu.edu) [16, 17]. In total, we identified 27 SNPs/Indels that were associated significantly with SIH ($P < 1 \times 10^{-5}$; Figure 2A and Table 1 and Figure S2 and Table S3). Among all these significant loci, 48.1% of them are located in the intronic region, 37.1% in the intergenic region or less than 1 kb downstream or upstream of an annotated gene and 14.8% were in the coding region (Figure 2B), which is comparable to the distribution of SNPs/Indels from previous studies in the DGRP [32].

Genes associated with SIH are enriched in molecular function GO terms related to ion channels and mRNA binding

A total of 18 genes were nominated (Table 2). To study if a particular molecular function was enriched in SIH, we performed gene enrichment analysis [21, 22]. Since 18 candidate genes with $P < 1 \times 10^{-5}$ in GWA were too few for gene enrichment analyses, we therefore used candidate genes with $P < 1 \times 10^{-4}$ in GWA instead (Table S4). We found that they were enriched in 54 GO terms (Table S5). Terms associated with more than five candidate genes were shown in Figure 2C. Among them, molecular function GO terms are cation channel activity (GO:0005261) and mRNA binding (GO:0003729), suggesting that genes with these two molecular functions are important for SIH.

In addition to GO analysis, we also grouped all significant candidate genes into five categories based on their known or predicted molecular functions from the fly database (flybase.org, Table 2). Category A includes genes encoding proteins with metabolic enzyme activities (3/18); Category B includes genes encoding proteins with binding activities to proteins or small molecules (4/18); Category C includes genes encoding proteins with receptor activities (2/18); Category D includes genes encoding proteins with nucleic acid (both DNA and RNA) binding activities (5/31). Lastly, Category E includes genes with so far unknown molecular functions (4/18).

We were most intrigued by genes encoding proteins that have mRNA binding activities since many mRNA binding proteins (RBPs) are splicing regulators for alternative pre-mRNA splicing, one of the important cellular responses that are often observed when cells/organisms are under starvation as well as other stresses [13, 14, 15]. Two genes that encode RNA binding proteins were shown in the list of nominated genes: *Syp* (*Syncrip*) and *shep* (*alan shepard*). We chose to validate gene *Syp* as the loss of *shep*, even only in neurons, can lead to abnormal locomotor activities in adult flies [33], which could complicate the final data interpretation.

Knockdown of *Syp* in neurons significantly affects SIH

To test whether gene *Syp* plays a role in SIH, we used the binary UAS/GAL4 system [34] to knock down its expression. We first crossed the gene-specific UAS-RNAi line with

Table 1. SNPs/Indels significantly associated with SIH variation at $P < 1 \times 10^{-5}$

SNP/INDEL	Minor Allele	Major Allele	Ref Allele	MAF	Effect size	*P* value	Nominated gene	FlybaseID	Site
X_7450403_SNP	T	A	A	0.05051	-285.1	1.69E-06	n/a	n/a	Intergenic
2L_16836590_SNP	A	T	T	0.07368	-239.4	3.37E-06	CG13283	FBgn0032613	Non-Synonymous
X_18534233_SNP	G	A	A	0.08763	-231.7	6.18E-07	*Rip11*	FBgn0027335	Intron
3R_16606144_SNP	T	G	G	0.08763	-211.5	2.66E-06	*Syp*	FBgn0038826	Intron
3R_16606324_SNP	A	G	G	0.08629	-206.7	5.57E-06	*Syp*	FBgn0038826	Intron
X_5324045_SNP	T	A	A	0.1399	-174	5.05E-06	CG15784	FBgn0029766	Upstream
X_5324047_SNP	T	C	C	0.1378	-173.5	5.24E-06	CG15784	FBgn0029766	Upstream
3L_5158751_SNP	A	T	T	0.2254	-162.5	1.24E-06	*shep*	FBgn0052423	Intron
3L_16130048_SNP	T	C	C	0.1943	-160.2	2.96E-06	CG16838	FBgn0036574	Synonymous
3L_10188818_SNP	A	T	T	0.2051	-153.5	2.70E-06	*ect*	FBgn0000451	Intron
2R_19671442_SNP	T	C	C	0.2073	-145.6	1.03E-05	CG9850	FBgn0034903	Intron
X_16205897_SNP	G	C	C	0.199	-145.4	1.43E-05	CG9915	FBgn0030738	Synonymous
2L_6464258_SNP	A	T	T	0.2778	-138.5	5.18E-06	CG16947	FBgn0031816	Intron
3L_16128605_SNP	G	T	T	0.2712	-135.9	9.81E-06	CG16838	FBgn0036574	Synonymous
2R_16523641_SNP	A	C	C	0.4294	-131.9	7.83E-06	*rig*	FBgn0250850	Intron
2L_1699735_SNP	A	C	C	0.2826	-130.1	6.50E-06	*chinmo*	FBgn0086758	Downstream
2L_1699738_SNP	C	A	A	0.2842	-128.7	8.02E-06	*chinmo*	FBgn0086758	Downstream
X_6643090_INS	ACA	A	A	0.4913	123.9	7.23E-06	CG14439	FBgn0029898	Intron
3R_11861018_DEL	ACT	A	ACT	0.497	127	1.37E-05	*pnr*	FBgn0003117	Intron
2L_1788750_SNP	C	T	C	0.3966	129.2	3.66E-06	*Gr22d*	FBgn0045498	Downstream
2L_1788739_INS	T	TT	T	0.3946	129.7	2.44E-06	*Gr22d*	FBgn0045498	Downstream
2L_1788747_SNP	A	C	A	0.3978	132.5	1.70E-06	*Gr22d*	FBgn0045498	Downstream
3L_5503742_SNP	T	G	G	0.3743	132.7	3.63E-06	CG34342	FBgn0085371	Intron
3R_15288909_SNP	G	A	A	0.3027	133.4	1.36E-05	*Dys*	FBgn0260003	Intron
2L_1788734_SNP	C	A	C	0.3944	133.4	1.68E-06	*Gr22d*	FBgn0045498	Downstream
3L_5503669_SNP	C	T	T	0.3487	135.2	2.31E-06	*CG34342*	FBgn0085371	Intron
3L_5505206_SNP	G	A	A	0.3333	146.8	1.33E-07	*Lkr*	FBgn0035610	Downstream

MAF, Minor Allele Frequency; Effect size, Effect size of Minor Allele

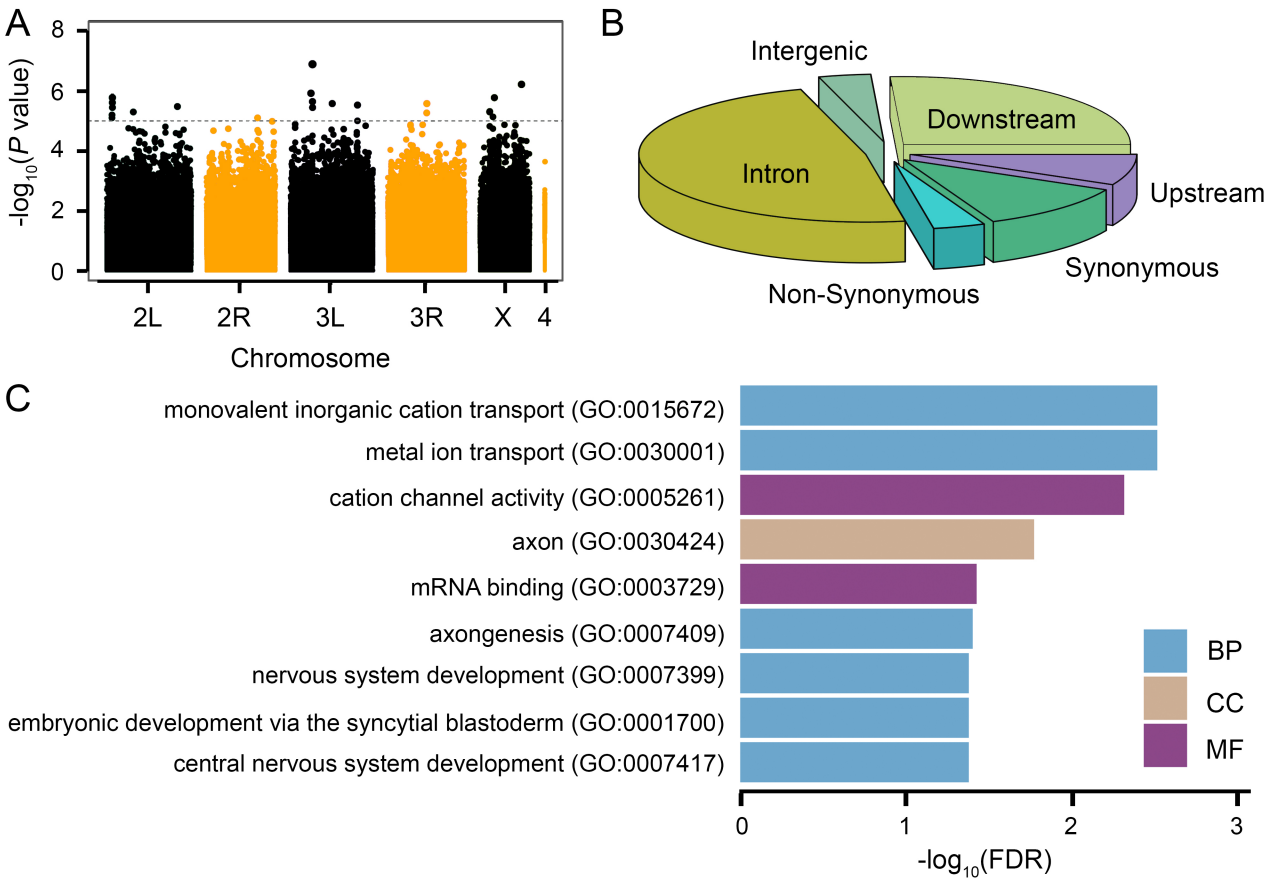

Figure 2. Manhattan plot for GWA, genomic location of significant SNPs, and Gene Ontology (GO) analysis. (A) Manhattan plot of SIH. The gray dotted line is the significant cutoff line used for gene nomination ($P < 1 \times 10^{-5}$). (B) Genomic location of significant SNPs/Indels. (C) GO terms associated with more than 5 genes. BP: Biological Process; CC: Cellular Component; MF: Molecular Function.

Table 2. Known or predicted molecular functions of nominated genes

Gene	Molecular Function	Category
CG34342	fatty acyl-CoA reductase (alcohol-forming) activity	Metabolic enzyme activity
CG13283	metalloendopeptidase activity	Metabolic enzyme activity
CG9850	metalloendopeptidase activity	Metabolic enzyme activity
CG16838	DNA binding activity	Nucleic acid binding activity
pnr	DNA binding transcription factor activity	Nucleic acid binding activity
shep	mRNA binding; RNA binding	Nucleic acid binding activity
Syp	mRNA binding; RNA binding	Nucleic acid binding activity
chinmo	nucleic acid binding	Nucleic acid binding activity
Dys	actin binding	Protein or small molecule binding activity
rig	protein binding	Protein or small molecule binding activity
Rip11	Rab GTPase binding	Protein or small molecule binding activity
CG16947	ubiquitin-protein transferase activity; Zinc ion binding	Protein or small molecule binding activity
Lkr	leucokinin receptor activity; Neuropeptide Y receptor activity	Receptor activity
Gr22d	taste receptor activity	Receptor activity
CG14439	n/a	Unknown function
CG15784	n/a	Unknown function
CG9915	n/a	Unknown function
ect	n/a	Unknown function

an *actin*-Gal4 driver to generate ubiquitous *Syp* knockdown flies. We observed that ubiquitous *Syp* knockdown led to lethality before the adult stage. This observation is consistent with previous studies showing that *Syp* mutant flies have highly decreased adult viability [35]. Given that *Syp* is highly expressed in adult heads (modENCODE.org), we therefore generated neuron-specific *Syp* knockdown flies by crossing UAS- *Syp* RNAi flies with a pan-neuronal driver *nSyb*-Gal4. Neuron-specific *Syp* knockdown flies did not exhibit lethality, suggesting that the fatality of ubiquitous *Syp* knockdown flies is likely due to the lack of expression of *Syp* in non-neuronal cells.

We then tested neuron-specific *Syp* knockdown and control flies in the Drosophila Activity Monitor under either food or starvation conditions. As shown in Figure 3A, neuron-specific *Syp* knockdown did not affect the locomotor activities in the food condition, suggesting that *Syp* in neurons is not required for the general locomotor activity. However, Delta Activity from them was significantly lower than that from control flies (Figure 3B), demonstrating a specific role of *Syp* in SIH. The reduced Delta Activity was also observed in neuron-specific *Syp* knockdown flies generated from another independent UAS- *Syp* RNAi line (Figure 3C and 3D). We therefore conclude that neuronal specific knock down of *Svp* impairs SIH.

Syp in adult neurons regulates Starvation-Induced Hyperactivity

Syp has been shown to affect the synaptic morphology and synaptic release at the neuromuscular junction in *Drosophila* larvae [36, 37]. Moreover, it has also been implicated in neuron/glia cell fate determination during development [38, 39]. The role of *Syp* in regulating SIH, therefore, could be due to its developmental effects. To study this possibility, we combined UAS-*Syp* RNAi with the Temporal and Regional Gene Expression Targeting (TARGET) system [34] to control the expression of RNAi temporally. The TARGET system consists of three elements: Gal4, UAS, and temperature sensitive Gal80 mutant (Gal80^{ts}). The Gal80^{ts} blocks Gal4-induced RNAi expression when tissue is exposed to the Gal80^{ts} permissive temperature (18°C). At a Gal80^{ts} restrictive temperature (31°C), Gal80^{ts} loses its binding to Gal4, which allows Gal4-dependent RNAi expression.

To bypass the developmental stage, we bred flies at 18°C until adult flies emerged. We then shifted the temperature of the incubator to 31°C and incubated adult flies in the new food vials for one more day, which was followed by behavioral testing at 31°C under both starvation and food conditions for three days (Figure 4A). To confirm *Syp* was indeed knocked down in adult flies, we compared the Syp protein level in adult fly heads from *Tub*-Gal80^{ts}/+; *nSyb*-Gal4/UAS-*Syp* RNAi (ts-Syp-KD) and +/+; *nSyb*-Gal4/UAS-*Syp* RNAi (Syp-KD) flies that were maintained at either 31°C or 18°C for two days. As shown in Figure 4B and 4C, at 31°C, the Syp level was comparable between two genotypes ($P = 0.4476$, n = 4 biological replicates per genotype; Figure S3). In comparison, at 18°C, the Syp level in ts-Syp-KD flies was about 20% higher than that in Syp-KD flies, presumably due to the binding of Gal80^{ts} to Gal4. The difference in the latter group is marginally significant ($P = 0.0496$); however, considering *Syp* was knocked down only in neurons and its protein level was examined in heads, which include both neuronal and non-neuronal cells, a lower magnitude of difference is expected.

Next, we examined the contribution of *Syp* in adult neurons to SIH. We monitored the locomotor activity of adult flies from ts-Syp-KD and also from other control genotypes (namely, +/+; *nSyb*-Gal4/+, *Tub*-Gal80^{ts}/+; UAS-*Syp* RNAi/+, and *Tub*-Gal80^{ts}/+; +/+) in the Drosophila Activity Monitor at 31°C for three days. We also included Syp-KD flies as positive controls. Flies from each genotype were tested under either food or starvation conditions. Results showed that ts-Syp-KD flies exhibited significantly attenuated SIH in comparison to control flies (Figure 4D and 4E), and that the Delta Activity level from ts-Syp-KD flies was comparable to that from Syp-KD flies ($P = 0.6863$). Taken together, we conclude that it is Syp in adult neurons that regulates SIH.

Syp is alternatively spliced upon starvation

Gene *Syp* spans a region of 54 kb in the genome, and it has 20 well documented splice variants (www.flybase.org, Figure 5). To study how *Syp* was regulated under starvation, we performed RNA sequencing (RNA-seq) on adult heads from wild-type flies (w^{1118}) reared under either food or starvation conditions (Figures S4-S6; see Methods for details). We first examined whether the *Syp* mRNA level was altered after starvation. Results from differential expression analyses showed that a total of 574 genes were down-regulated, and a total of 84 genes were up-regulated under starvation (Criteria applied: false-discovery rate (FDR) < 0.05 and fold change ≥ 2 or fold change $\leq$ -2; Figure S7 and Table S6). Gene *Syp* was not on the list, suggesting that its expression was not dramatically regulated by starvation. This conclusion was further corroborated by similar protein levels of *Syp* under two conditions (Figure S8). To examine the function of down- or up-regulated genes, we performed gene enrichment analyses for each list of genes. We found that down-regulated genes participated in a variety of metabolic pathways, whereas up-regulated genes were mainly enriched in pathways related to DNA repair, nutrients recycling, and spliceosome (Figure S7). The fact that genes involved in the spliceosome are upregulated upon starvation suggests that alternative splicing may underlie responses to starvation.

To find out genes that underwent alternative splicing under starvation, we analyzed RNA-seq data using LeafCutter, a software that can identify and quantify both novel and known alternative splicing events [29]. LeafCutter focuses on intron excisions and groups RNA-seq reads into different clusters based on their mapped location to the genome. Therefore, the final data presentation is in the form of clusters that include various splicing forms. A cluster was considered significant

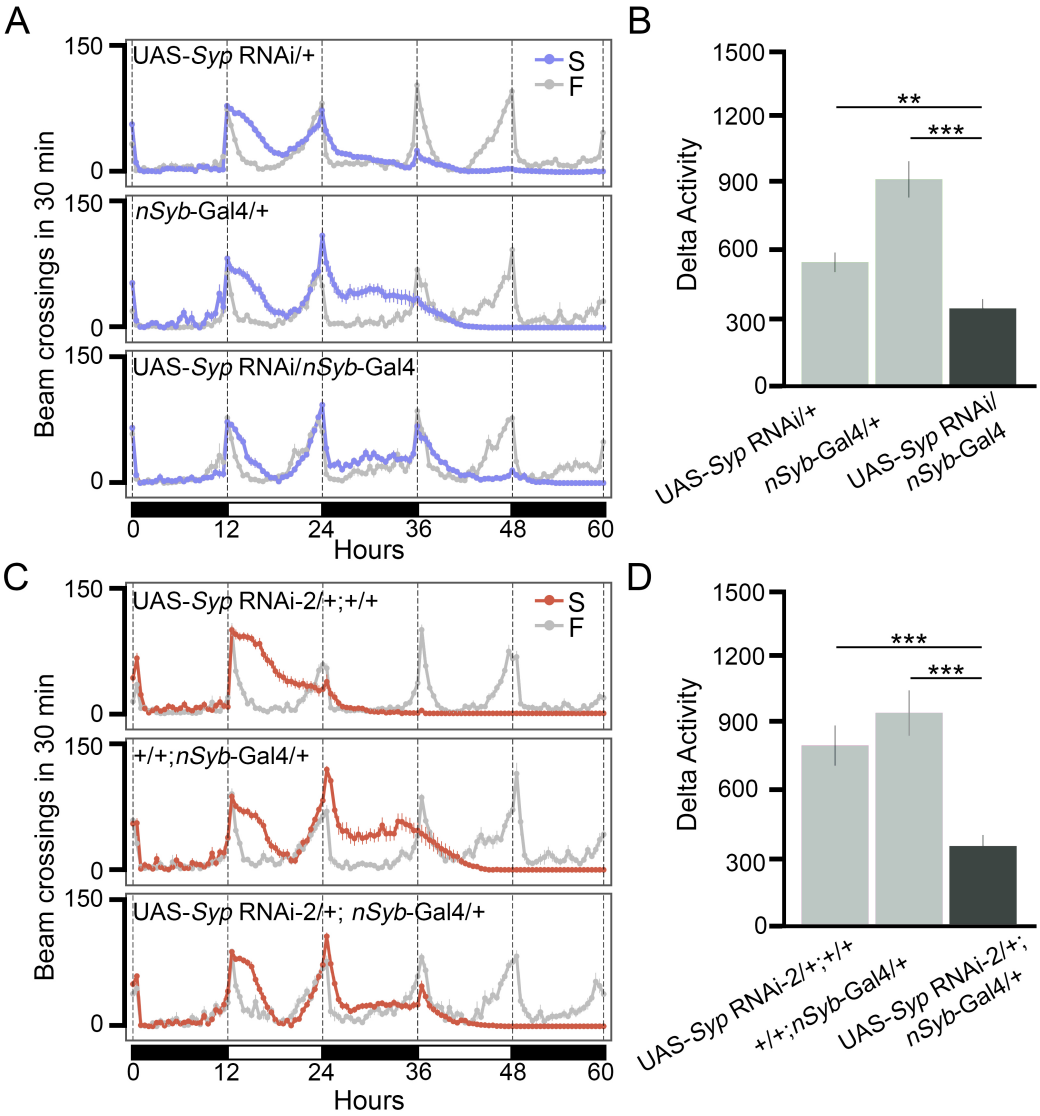

Figure 3. Knocking down of *Syp* in neurons reduces SIH. (A) Locomotor activity responses to starvation from neuron-specific *Syp* knockdown flies (genotype: UAS-*Syp* RNAi/*nSyb*-Gal4) and two parental control lines (genotypes: UAS-*Syp* RNAi/+ and *nSyb*-Gal4/+, respectively). Gray lines represent activities under the food condition (F) and purple lines represent activities under the starvation condition (S). Black and white bars at the bottom of the panel represent night and day cycles, respectively. n = 16-20 per genotype per condition. (B) Summary plot of SIH in panel A. (C) Locomotor activity responses to starvation from neuron-specific *Syp* knockdown flies generated from a second RNAi line (genotype: UAS-*Syp* RNAi-2/+; *nSyb*-Gal4/+) and two parental control lines (genotypes: UAS-*Syp* RNAi-2/+; +/+ and +/+; *nSyb*-Gal4/+, respectively). n = 20-24 per genotype per condition. (D) Summary plot of SIH in panel C. ** $P < 0.01$, *** $P < 0.001$, unpaired *t*-test with Bonferroni Correction. Error bars represent SEM.

when FDR < 0.05. A total of 1927 clusters from 359 genes were alternatively spliced under starvation (Table S7). Gene enrichment analyses showed that these genes were implicated in a variety of biological processes, including regulation of mRNA splicing (Table S8). Remarkably, the most significant molecular function GO term is mRNA binding (Figure S9 and Table S8), suggesting that upon starvation, genes encode RNA-binding proteins tend to be alternatively spliced.

Among these 1927 significant clusters, 359 of them, from 180 genes, have a ΔPSI larger than 10%. PSI, Percentage Sliced In, is the fraction of a geneâs mRNAs that contain the exon; therefore, ΔPSI is the difference in PSI between the starvation condition and the food condition. Among these 359 clusters, 80.8% of them have small splicing changes (10% $<$ ΔPSI $<$25%), 18.7% of them have intermediate splicing changes (25% $\leq$ ΔPSI $\leq$ 50%), and 0.5% of them have large splicing changes (ΔPSI $>$ 50%). As expected, gene *Syp* is alternatively spliced under starvation (Table S7).

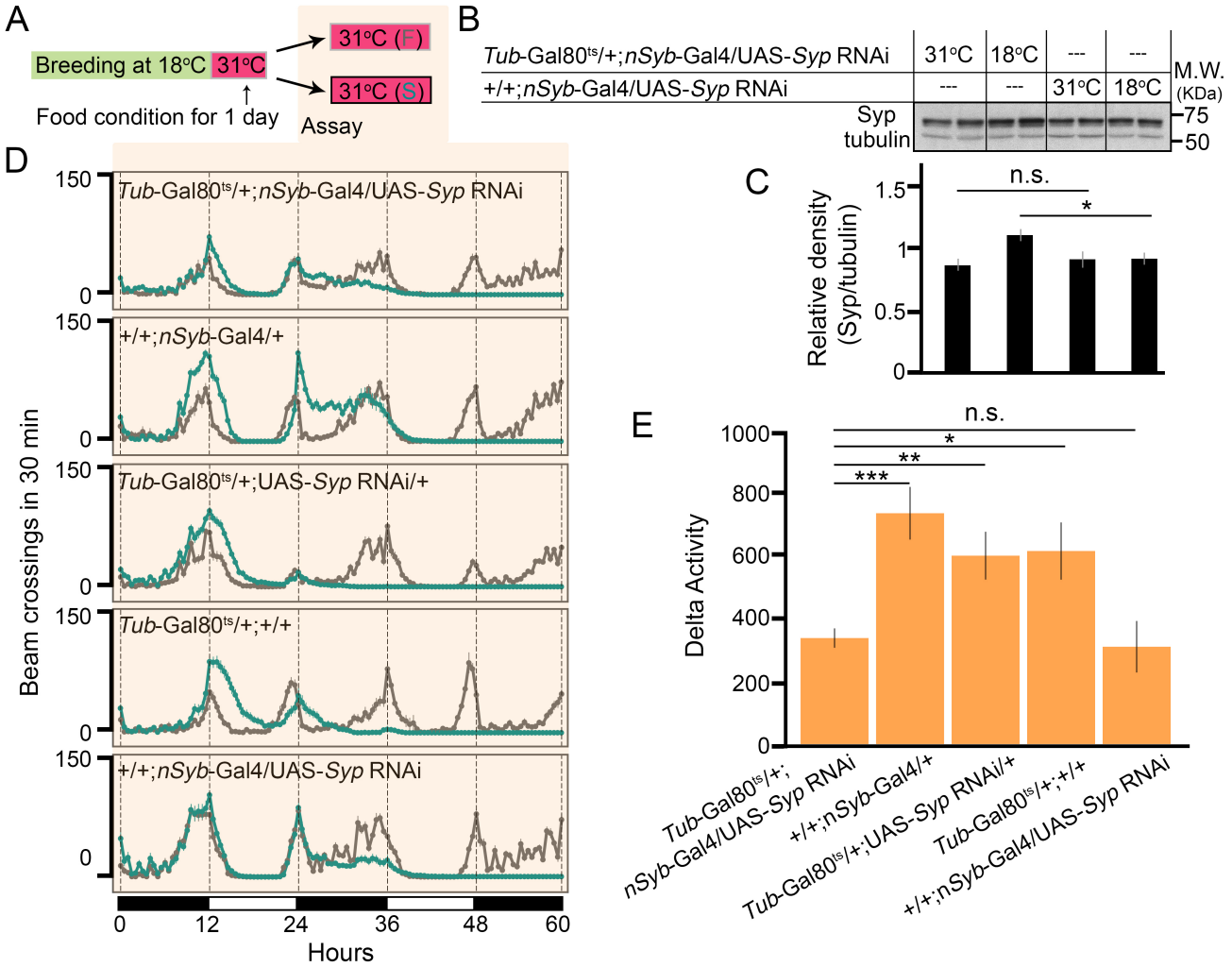

Figure 4. Syp in adult neurons regulates SIH.(A) Breeding and testing scheme. F: food condition; S: starvation condition. (B) Western blot of adult fly head homogenate from *Tub*-Gal80^{ts}/+;*nSyb*-Gal4/UAS-*Syp* RNAi (ts-Syp-KD) and +/+;*nSyb*-Gal4/UAS-*Syp* RNAi (Syp-KD) flies. Two biological replicates per genotype per condition. Tubulin is the loading control. (C) Quantification of Syp from four biological replicates (see Figure S3 for the other two replicates). (D) Locomotor activity responses to starvation from each genotype. n = 24-30 per genotype per condition. (E) Summary plot of SIH from each genotype in panel D. * $P < 0.05$, ** $P < 0.01$, *** $P < 0.001$, n.s: $P > 0.05$, unpaired *t*-test with Bonferroni Correction. Error bars represent SEM.

A total of 10 splicing events were included in this significant cluster. Among them, the top two ΔPSIs were -0.12 and 0.06 (Figure 5A). The splice variants that correspond to the changes are Syp-RI (Transcript ID: FBtr0334711), Syp-RR (FBtr0334720), Syp-RO (FBtr0334717), Syp-RA (FBtr0083958), Syp-RH (FBtr0113256), Syp-RC (FBtr0083960), Syp-RF (FBtr0083961), and Syp-RE (FBtr0083963) (Figure 5B). To confirm that these changes were not from sequencing noises, we designed PCR primers to target the middle exons within this region (exons b and c, Figure 5A) and performed qRT-PCR. Results showed that the expression of the middle two exons in starved flies was reduced to 38% of that in flies maintained under the food condition (Figure 5C), which confirmed the increased splicing from exon a to exon d. We further designed primers to target exon b only and found that the expression of exon b was unchanged after starvation (Figure 5C), which was expected since this exon was involved in two splicing events that were regulated in opposite directions by starvation.

Discussion

Starvation-Induced Hyperactivity (SIH) has been observed in different species [3, 4, 5, 6, 7, 8, 9, 10, 11, 12], suggesting that it has a genetic component. Taking advantage of the genetic diversity in the DGRP strains derived from a wild population, we have demonstrated for the first time the significant contribution of the genetic component to SIH. Our studies show that the broad sense of heritability (H^2) of SIH is 0.38, which

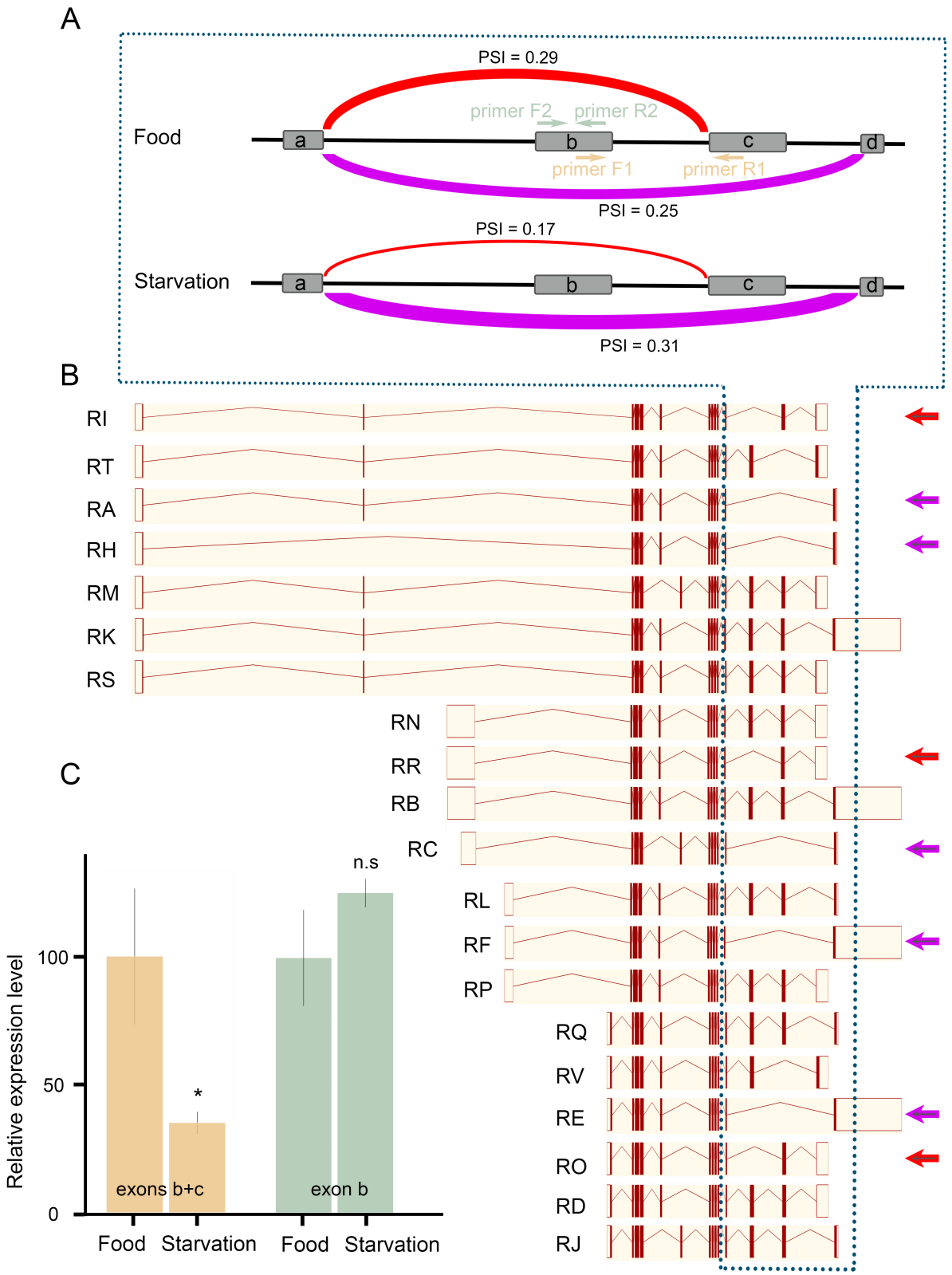

Figure 5. *Syp* is alternatively spliced under starvation. (A) Differential usage of exons in *Syp* under food and starvation conditions. Four exons involved in the alternative splicing were shown and referred to as exon a, exon b, exon c, and exon d. PSI: Percentage Sliced In. (B) Various splice variants of *Syp* (www.flybase.org). Arrows indicate splice variants that were either downregulated (red color) or upregulated (purple) under starvation. (C) Relative expression of targeted exons measured by qPCR. The targeted locations of each pair of primers were indicated in panel A. * $P < 0.05$, n.s: $P > 0.05$, unpaired t-test, n = 4 per condition. Error bars represent SEM.

is lower than developmental traits examined in the DGRP (e.g. H^2 is 0.89, 0.66-0.88, and 0.71-0.78 for developmental time [40], pigmentation [41], and wing morphology [42], respectively), but is on the high end for behavioral traits (e.g. H^2 is 0.03-0.09 and 0.02-0.45 for courtship behavior [43] and olfactory behavior [44, 45, 46], respectively), suggesting that SIH has a strong genetic basis among various behavioral traits.

We further performed genome-wide association studies and identified 27 loci from 18 genes significantly associated with SIH in adult *Drosophila*. Gene enrichment analyses revealed that both ion channels and mRNA binding proteins were important for SIH. We validated the role of *Syp* in adult neurons in regulating SIH and showed that specific *Syp* transcripts were responsible for SIH. Syp is a Drosophila homolog of human SYNaptotagmin-binding Cytoplasmic RNA-Interacting Protein (SYNCRIP)/hnRNP Q, and they share 47% sequence identity [35]. Similar to the mammalian SYNCRIP, Syp consists of three RNA recognition motifs and one acidic domain at the N-terminus [35, 47]. However, it lacks the arginine-glycine-glycine domain at the C-terminus [35]. In mammals, different domains mediate the interaction of SYNCRIP with different effectors, which renders SYNCRIP a wide range of functions including circadian regulation [48, 49, 50], neuronal morphogenesis [51, 52, 53], and stress response [54]. Misregulation of SYNCRIP has been reported in neurodegenerative diseases [55, 56], psychiatric disorders [57, 58], and cancer [59, 60]. In flies, studies have shown that Syp is required for different developmental phenotypes, such as oogenesis [35], maintaining a normal structure and function of synapses at the neuromuscular junction in larvae [36, 37], and determining neuron/glia cell fates [38, 39]. Our studies demonstrate for the first time that Syp has a unique function in adult flies (Figure 3), and this function is independent of its developmental effects (Figure 4). It remains unknown how the Syp protein regulates SIH in adult *Drosophila* at the molecular level. Previous studies indicate that Syp, at the *Drosophila* larval neuromuscular junction, can modulate the presynaptic vesicle release through regulating postsynaptic translation [37] and can regulate activity-dependent synaptic plasticity [61]. Similar functions have also been observed in mammalian SYNCRIP such that it is a component of neuronal RNA transport granules that can regulate dendritic morphology [51, 62, 63, 64], and that it inhibits translation by competing with the poly(A) binding protein [65]. Thus, it is reasonable to speculate that Syp might be able to quickly affect protein synthesis in neurons and even local protein synthesis in synapses in response to starvation. Further studies are needed to examine the molecular and neural mechanisms associated with Syp in adult neurons in response to starvation.

Although the function of *Syp* has been explored in different contexts [35, 36, 37, 38, 39], the functional significance of its transcriptional or post-transcriptional regulation was seldom studied. Our results from RNA-seq suggest that under starvation, *Syp* is mainly regulated at the post-transcriptional level, and that specific variants are responsible for SIH (Figure 5). It will be of interest to identify the upstream molecules that affect the splicing of *Syp* under starvation. Previous studies have shown that there is a cross-regulatory network where one RNA-binding protein can regulate the alternative splicing of other RNA-binding proteins [66]. This is also implicated in our splice variants analysis followed by GO analysis. Genes encoding RBPs seem to be especially regulated by alternative splicing.

The SIH gene list has been expanding in recent years, which includes *Sirt1* [11], *AMP-activated protein kinase* (*AMPK*) [5, 6], *Adipokinetic hormone* (*Akh*) [4], *Adipokinetic hormone receptor* (*AkhR*) [8], *Insulin-like peptides* (*Ilps*) [8], *Insulin-like receptor* (*InR*) [8], *Tyramine beta hydroxylase* (*Tbh*) [7], and *dG9a* [9]. This study further adds *Syp*, which encodes an RNA-binding protein (RBP), to the list. It remains to be determined whether other candidates from this GWA study also affect SIH. It is worth to mention that none of those previously reported SIH genes were candidates in the present GWA study, which is likely due to the limited genetic diversity in the DGRP strains [18].

Starvation is one of the most common environment stresses faced by animals living in the wild. Previous studies have shown that starvation can profoundly affect gene expression at the transcriptional level [67, 68], the present study further demonstrate that starvation can also affect post-transcription regulations such as alternative splicing. Our RNA-seq data indicate that only 15 genes (3 up-regulated and 12 down-regulated) are shared between the 658 differentially expressed genes and the 180 alternatively spliced genes, suggesting that regulation at both transcriptional are post-transcriptional levels for the same gene is uncommon in response to starvation, at least in the head tissue. Gene enrichment analyses further suggest that metabolic genes tend to be regulated at the transcriptional level while genes involved in the mRNA regulation tend to be regulated post-transcriptionally.

Acknowledgments

We thank Ilan Davis for sharing the anti-Syp antibody. We thank Chunyu Liu and Xiaochang Zhang for helpful discussions. We thank Wei A. Du and Meredith Wells for technical assistance. We thank the Bloomington Drosophila Stock Center (BDSC) and the Vienna Drosophila Resource Center (VDRC) for fly stocks. The computational analysis in this study was performed with resources provided by the University of Chicagoâs Research Computing Center. This work was supported by the National Institutes of Health (T32MH020065 & T32DA434693 to W.C., R01GM100768 to X.Z.).

Author contributions

W.C., E.S.H., and X.Z. designed research; W.C., W.L., and W.F. performed research; W.C. analyzed data; W.C. and X.Z. wrote the paper. All authors edited the manuscript.

Conflict of Interest Statement

The authors declare no conflict of interest.

References

[1] Marshall D McCue. Starvation physiology: reviewing the different strategies animals use to survive a common challenge. *Comparative Biochemistry and Physiology Part A: Molecular & Integrative Physiology*, 156(1):1–18, 2010.

[2] Daowei Zhang, Zhongjiu Xiao, Boping Zeng, Kun Li, and Yanlong Tang. Insect behavior and physiological adaptation mechanisms under starvation stress. *Frontiers in physiology*, 10:163, 2019.

[3] KJ Connolly. Locomotor activity in drosophila as a function of food deprivation. *Nature*, 209(5019):224, 1966.

[4] Gyunghee Lee and Jae H Park. Hemolymph sugar homeostasis and starvation-induced hyperactivity affected by genetic manipulations of the adipokinetic hormone-encoding gene in drosophila melanogaster. *Genetics*, 167(1):311–323, 2004.

[5] Erik C Johnson, Nevzat Kazgan, Colin A Bretz, Lawrence J Forsberg, Clare E Hector, Ryan J Worthen, Rob Onyenwoke, and Jay E Brenman. Altered metabolism and persistent starvation behaviors caused by reduced ampk function in drosophila. *PLoS One*, 5(9):e12799, 2010.

[6] Jason T Braco, Emily L Gillespie, Gregory E Alberto, Jay E Brenman, and Erik C Johnson. Energy-dependent modulation of glucagon-like signaling in drosophila via the amp-activated protein kinase. *Genetics*, 192(2):457–466, 2012.

[7] Zhe Yang, Yue Yu, Vivian Zhang, Yinjun Tian, Wei Qi, and Liming Wang. Octopamine mediates starvation-induced hyperactivity in adult drosophila. *Proceedings of the National Academy of Sciences*, 112(16):5219–5224, 2015.

[8] Yue Yu, Rui Huang, Jie Ye, Vivian Zhang, Chao Wu, Guo Cheng, Junling Jia, and Liming Wang. Regulation of starvation-induced hyperactivity by insulin and glucagon signaling in adult drosophila. *Elife*, 5:e15693, 2016.

[9] Kouhei Shimaji, Ryo Tanaka, Toru Maeda, Mamiko Ozaki, Hideki Yoshida, Yasuyuki Ohkawa, Tetsuya Sato, Mikita Suyama, and Masamitsu Yamaguchi. Histone methyltransferase g9a is a key regulator of the starvation-induced behaviors in drosophila melanogaster. *Scientific reports*, 7(1):14763, 2017.

[10] K My Pirke, A Broocks, T Wilckens, R Marquard, and U Schweiger. Starvation-induced hyperactivity in the rat: the role of endocrine and neurotransmitter changes. *Neuroscience & Biobehavioral Reviews*, 17(3):287–294, 1993.

[11] Danica Chen, Andrew D Steele, Susan Lindquist, and Leonard Guarente. Increase in activity during calorie restriction requires sirt1. *Science*, 310(5754):1641–1641, 2005.

[12] Zhi-Jun Zhao, Ke-Xin Chen, Yong-An Liu, Chun-Ming Wang, and Jing Cao. Decreased circulating leptin and increased neuropeptide y gene expression are implicated in food deprivation-induced hyperactivity in striped hamsters, cricetulus barabensis. *Hormones and behavior*, 65(4):355–362, 2014.

[13] Martin Dutertre, Gabriel Sanchez, Jérôme Barbier, Laurent Corcos, and Didier Auboeuf. The emerging role of pre-messenger rna splicing in stress responses: sending alternative messages and silent messengers. *RNA biology*, 8(5):740–747, 2011.

[14] Jeffrey A Pleiss, Gregg B Whitworth, Megan Bergkessel, and Christine Guthrie. Rapid, transcript-specific changes in splicing in response to environmental stress. *Molecular cell*, 27(6):928–937, 2007.

[15] Lisa M Salati and Batoul Amir-Ahmady. Dietary regulation of expression of glucose-6-phosphate dehydrogenase. *Annual review of nutrition*, 21(1):121–140, 2001.

[16] Trudy FC Mackay, Stephen Richards, Eric A Stone, Antonio Barbadilla, Julien F Ayroles, Dianhui Zhu, Sònia Casillas, Yi Han, Michael M Magwire, Julie M Cridland, et al. The drosophila melanogaster genetic reference panel. *Nature*, 482(7384):173, 2012.

[17] Wen Huang, Andreas Massouras, Yutaka Inoue, Jason Peiffer, Miquel Ràmia, Aaron M Tarone, Lavanya Turlapati, Thomas Zichner, Dianhui Zhu, Richard F Lyman, et al. Natural variation in genome architecture among 205 drosophila melanogaster genetic reference panel lines. *Genome research*, 24(7):1193–1208, 2014.

[18] Trudy FC Mackay and Wen Huang. Charting the genotype–phenotype map: lessons from the drosophila melanogaster genetic reference panel. *Wiley Interdisciplinary Reviews: Developmental Biology*, 7(1):e289, 2018.

[19] Steven J Marygold, Paul C Leyland, Ruth L Seal, Joshua L Goodman, Jim Thurmond, Victor B Strelets, Robert J Wilson, and FlyBase Consortium. Flybase: improvements to the bibliography. *Nucleic acids research*, 41(D1):D751–D757, 2012.

[20] Sean E McGuire, Zhengmei Mao, and Ronald L Davis. Spatiotemporal gene expression targeting with the target and gene-switch systems in drosophila. *Sci. STKE*, 2004(220):pl6–pl6, 2004.

[21] Edward Y Chen, Christopher M Tan, Yan Kou, Qiaonan Duan, Zichen Wang, Gabriela Vaz Meirelles, Neil R Clark, and Avi Ma'ayan. Enrichr: interactive and collaborative html5 gene list enrichment analysis tool. *BMC bioinformatics*, 14(1):128, 2013.

[22] Maxim V Kuleshov, Matthew R Jones, Andrew D Rouillard, Nicolas F Fernandez, Qiaonan Duan, Zichen Wang, Simon Koplev, Sherry L Jenkins, Kathleen M Jagodnik, Alexander Lachmann, et al. Enrichr: a comprehensive gene set enrichment analysis web server 2016 update. *Nucleic acids research*, 44(W1):W90–W97, 2016.

[23] K Dolinski, SS Dwight, JT Eppig, MA Harris, DP Hill, L Issel-Tarver, A Kasarskis, S Lewis, JC Matese, JE Richardson, et al. Gene ontology: tool for the unification of biology. the gene ontology consortium. *Nat Genet*, 25(1):2529Attri, 2000.

[24] Hiroyuki Ogata, Susumu Goto, Kazushige Sato, Wataru Fujibuchi, Hidemasa Bono, and Minoru Kanehisa. Kegg: Kyoto encyclopedia of genes and genomes. *Nucleic acids research*, 27(1):29–34, 1999.

[25] Simon Andrews et al. Fastqc: a quality control tool for high throughput sequence data, 2010.

[26] A Dobin, CA Davis, F Schlesinger, J Drenkow, C Zaleski, S Jha, P Batut, M Chaisson, and TR Gingeras. Star: ultrafast universal rna-seq aligner. bioinformatics29, 15–21, 2013.

[27] E Mancini, J Iserte, M Yanovsky, and A Chernomoretz. Aspli: analysis of alternative splicing using rna-seq. *Bioconductor: R package version*, 1(3), 2017.

[28] H Li, B Handsaker, A Wysoker, T Fennell, J Ruan, N Homer, G Marth, G Abecasis, and R Durbin. .(2009): The sequence alignment/map format and samtools. *Bioinformatics*, 25(16):2078–2079, 2009.

[29] Yang I Li, David A Knowles, Jack Humphrey, Alvaro N Barbeira, Scott P Dickinson, Hae Kyung Im, and Jonathan K Pritchard. Annotation-free quantification of rna splicing using leafcutter. *Nature genetics*, 50(1):151, 2018.

[30] JC Hall. Genetics and molecular biology of rhythms in drosophila and other insects. *Advances in genetics*, 48:1, 2003.

[31] Yuh Chwen G Lee, Qian Yang, Wanhao Chi, Susie A Turkson, Wei A Du, Claus Kemkemer, Zhao-Bang Zeng, Manyuan Long, and Xiaoxi Zhuang. Genetic architecture of natural variation underlying adult foraging behavior that is essential for survival of drosophila melanogaster. *Genome biology and evolution*, 9(5):1357–1369, 2017.

[32] Susan T Harbison, Lenovia J McCoy, and Trudy FC Mackay. Genome-wide association study of sleep in drosophila melanogaster. *BMC genomics*, 14(1):281, 2013.

[33] Dahong Chen, Chunjing Qu, Sonia M Bjorum, Kathleen M Beckingham, and Randall S Hewes. Neuronal remodeling during metamorphosis is regulated by the alan shepard (shep) gene in drosophila melanogaster. *Genetics*, 197(4):1267–1283, 2014.

[34] Andrea H Brand and Norbert Perrimon. Targeted gene expression as a means of altering cell fates and generating dominant phenotypes. *development*, 118(2):401–415, 1993.

[35] Suzanne M McDermott, Carine Meignin, Juri Rappsilber, and Ilan Davis. Drosophila syncrip binds the gurken mrna localisation signal and regulates localised transcripts during axis specification. *Biology open*, 1(5):488–497, 2012.

[36] Suzanne M McDermott, Lu Yang, James M Halstead, Russell S Hamilton, Carine Meignin, and Ilan Davis. Drosophila syncrip modulates the expression of mrnas encoding key synaptic proteins required for morphology at the neuromuscular junction. *Rna*, 20(10):1593–1606, 2014.

[37] James M Halstead, Yong Qi Lin, Lita Durraine, Russell S Hamilton, Graeme Ball, Greg G Neely, Hugo J Bellen, and Ilan Davis. Syncrip/hnrnp q influences synaptic transmission and regulates bmp signaling at the drosophila neuromuscular synapse. *Biology open*, 3(9):839–849, 2014.

[38] Zhiyong Liu, Ching-Po Yang, Ken Sugino, Chi-Cheng Fu, Ling-Yu Liu, Xiaohao Yao, Luke P Lee, and Tzumin Lee. Opposing intrinsic temporal gradients guide neural stem cell production of varied neuronal fates. *Science*, 350(6258):317–320, 2015.

[39] Mubarak Hussain Syed, Brandon Mark, and Chris Q Doe. Steroid hormone induction of temporal gene expression in drosophila brain neuroblasts generates neuronal and glial diversity. *Elife*, 6:e26287, 2017.

[40] Barbara Horváth, Andrea J Betancourt, and Alex T Kalinka. A novel method for quantifying the rate of embryogenesis uncovers considerable genetic variation for the duration of embryonic development in drosophila melanogaster. *BMC evolutionary biology*, 16(1):200, 2016.

[41] Lauren M Dembeck, Wen Huang, Michael M Magwire, Faye Lawrence, Richard F Lyman, and Trudy FC Mackay. Genetic architecture of abdominal pigmentation in drosophila melanogaster. *PLoS genetics*, 11(5):e1005163, 2015.

[42] Sibylle Chantal Vonesch, David Lamparter, Trudy FC Mackay, Sven Bergmann, and Ernst Hafen. Genome-wide analysis reveals novel regulators of growth in drosophila melanogaster. *PLoS genetics*, 12(1):e1005616, 2016.

[43] Bryn E Gaertner, Elizabeth A Ruedi, Lenovia J McCoy, Jamie M Moore, Mariana F Wolfner, and Trudy FC Mackay. Heritable variation in courtship patterns in drosophila melanogaster. *G3: Genes, Genomes, Genetics*, 5(4):531–539, 2015.

[44] Shilpa Swarup, Wen Huang, Trudy FC Mackay, and Robert RH Anholt. Analysis of natural variation reveals

neurogenetic networks for drosophila olfactory behavior. *Proceedings of the National Academy of Sciences*, 110(3):1017–1022, 2013.

[45] EB Brown, JE Layne, C Zhu, AG Jegga, and SM Rollmann. Genome-wide association mapping of natural variation in odour-guided behaviour in drosophila. *Genes, Brain and Behavior*, 12(5):503–515, 2013.

[46] Gunjan H Arya, Michael M Magwire, Wen Huang, Yazmin L Serrano-Negron, Trudy FC Mackay, and Robert RH Anholt. The genetic basis for variation in olfactory behavior in drosophila melanogaster. *Chemical senses*, 40(4):233–243, 2015.

[47] Christine Beuck, James R Williamson, Kurt Wüthrich, and Pedro Serrano. The acidic domain is a unique structural feature of the splicing factor syncrip. *Protein Science*, 25(8):1545–1550, 2016.

[48] Do-Yeon Kim, Eunyee Kwak, Sung-Hoon Kim, Kyung-Ha Lee, Kyung-Chul Woo, and Kyong-Tai Kim. hnrnp q mediates a phase-dependent translation-coupled mrna decay of mouse period3. *Nucleic acids research*, 39(20):8901–8914, 2011.

[49] Kyung-Ha Lee, Kyung-Chul Woo, Do-Yeon Kim, Tae-Don Kim, Jaecheon Shin, Sung Mi Park, Sung Key Jang, and Kyong-Tai Kim. Rhythmic interaction between period1 mrna and hnrnp q leads to circadian time-dependent translation. *Molecular and cellular biology*, 32(3):717–728, 2012.

[50] Ilgye Lim, Youngseob Jung, Do-Yeon Kim, and Kyong-Tai Kim. Hnrnp q has a suppressive role in the translation of mouse cryptochrome1. *PloS one*, 11(7):e0159018, 2016.

[51] Hung-Hsi Chen, Hsin-I Yu, Wen-Cheng Chiang, Yu-De Lin, Ben-Chang Shia, and Woan-Yuh Tarn. hnrnp q regulates cdc42-mediated neuronal morphogenesis. *Molecular and cellular biology*, 32(12):2224–2238, 2012.

[52] Lei Xing, Xiaodi Yao, Kathryn R Williams, and Gary J Bassell. Negative regulation of rhoa translation and signaling by hnrnp-q1 affects cellular morphogenesis. *Molecular biology of the cell*, 23(8):1500–1509, 2012.

[53] Kathryn R Williams, Damian S McAninch, Snezana Stefanovic, Lei Xing, Megan Allen, Wenqi Li, Yue Feng, Mihaela Rita Mihailescu, and Gary J Bassell. hnrnp-q1 represses nascent axon growth in cortical neurons by inhibiting gap-43 mrna translation. *Molecular biology of the cell*, 27(3):518–534, 2016.

[54] DY Kim, W Kim, KH Lee, Sun-Hee Kim, HR Lee, HJ Kim, Y Jung, JH Choi, and KT Kim. hnrnp q regulates translation of p53 in normal and stress conditions. *Cell Death & Differentiation*, 20(2):226–234, 2013.

[55] Zissimos Mourelatos, Linda Abel, Jeongsik Yong, Naoyuki Kataoka, and Gideon Dreyfuss. Smn interacts with a novel family of hnrnp and spliceosomal proteins. *The EMBO journal*, 20(19):5443–5452, 2001.

[56] Federica Rizzo, Monica Nizzardo, Shikha Vashisht, Erika Molteni, Valentina Melzi, Michela Taiana, Sabrina Salani, Pamela Santonicola, Elia Di Schiavi, Monica Bucchia, et al. Key role of smn/syncrip and rna-motif 7 in spinal muscular atrophy: Rna-seq and motif analysis of human motor neurons. *Brain*, 142(2):276–294, 2019.

[57] Stefan H Lelieveld, Margot RF Reijnders, Rolph Pfundt, Helger G Yntema, Erik-Jan Kamsteeg, Petra de Vries, Bert BA de Vries, Marjolein H Willemsen, Tjitske Kleefstra, Katharina Löhner, et al. Meta-analysis of 2,104 trios provides support for 10 new genes for intellectual disability. *Nature neuroscience*, 19(9):1194, 2016.

[58] Hui Guo, Michael H Duyzend, Bradley P Coe, Carl Baker, Kendra Hoekzema, Jennifer Gerdts, Tychele N Turner, Michael C Zody, Jennifer S Beighley, Shwetha C Murali, et al. Genome sequencing identifies multiple deleterious variants in autism patients with more severe phenotypes. *Genetics in Medicine*, 21(7):1611–1620, 2019.

[59] Ly P Vu, Camila Prieto, Elianna M Amin, Sagar Chhangawala, Andrei Krivtsov, M Nieves Calvo-Vidal, Timothy Chou, Arthur Chow, Gerard Minuesa, Sun Mi Park, et al. Functional screen of msi2 interactors identifies an essential role for syncrip in myeloid leukemia stem cells. *Nature genetics*, 49(6):866, 2017.

[60] Stéphanie Gachet, Tiama El-Chaar, David Avran, Eulàlia Genescà, Frédéric Catez, Samuel Quentin, Marc Delord, Gabriel Thérizols, Delphine Briot, Godelieve Meunier, et al. Deletion 6q drives t-cell leukemia progression by ribosome modulation. *Cancer discovery*, 8(12):1614–1631, 2018.

[61] Josh Titlow, Francesca Robertson, Aino Järvelin, David Ish-Horowicz, Carlas Smith, Enrico Gratton, and Ilan Davis. Syncrip/hnrnpq is required for activity-induced msp300/nesprin-1 expression and new synapse formation. *bioRxiv*, page 585679, 2019.

[62] Hiroko Bannai, Kazumi Fukatsu, Akihiro Mizutani, Tohru Natsume, Shun-ichiro Iemura, Tohru Ikegami, Takafumi Inoue, and Katsuhiko Mikoshiba. An rna-interacting protein, syncrip (heterogeneous nuclear ribonuclear protein q1/nsap1) is a component of mrna granule transported with inositol 1, 4, 5-trisphosphate receptor type 1 mrna in neuronal dendrites. *Journal of Biological Chemistry*, 279(51):53427–53434, 2004.

[63] Y Kanai. Dohmae n, hirokawa n. *Kinesin transports RNA: isolation and characterization of an RNA-transporting granule. Neuron*, 43:513–525, 2004.

[64] George Elvira, Sylwia Wasiak, Vanessa Blandford, Xin-Kang Tong, Alexandre Serrano, Xiaotang Fan, Maria del Rayo Sanchez-Carbente, Florence Servant, Alexander W Bell, Daniel Boismenu, et al. Characterization of an rna

granule from developing brain. *Molecular & cellular proteomics*, 5(4):635–651, 2006.

[65] Yuri V Svitkin, Akiko Yanagiya, Alexey E Karetnikov, Tommy Alain, Marc R Fabian, Arkady Khoutorsky, Sandra Perreault, Ivan Topisirovic, and Nahum Sonenberg. Control of translation and mirna-dependent repression by a novel poly (a) binding protein, hnrnp-q. *PLoS biology*, 11(5):e1001564, 2013.

[66] Angela N Brooks, Michael O Duff, Gemma May, Li Yang, Mohan Bolisetty, Jane Landolin, Ken Wan, Jeremy Sandler, Benjamin W Booth, Susan E Celniker, et al. Regulation of alternative splicing in drosophila by 56 rna binding proteins. *Genome research*, 25(11):1771–1780, 2015.

[67] Ingo Zinke, Christina S Schütz, Jörg D Katzenberger, Matthias Bauer, and Michael J Pankratz. Nutrient control of gene expression in drosophila: microarray analysis of starvation and sugar-dependent response. *The EMBO journal*, 21(22):6162–6173, 2002.

[68] Susan T Harbison, Sherman Chang, Kim P Kamdar, and Trudy FC Mackay. Quantitative genomics of starvation stress resistance in drosophila. *Genome biology*, 6(4):R36, 2005.